INTRA-VEHICLE UWB CHANNELS IN MOVING AND STAIONARY SCENARIOS

Weihong Niu, Jia Li
ECE Department
Oakland University

and

Timothy Talty
General Motors Corporation
Warren, MI

ABSTRACT

This paper presents the ultra-wideband (UWB) channel measurement and modeling for an intra-vehicle environment. The measurement was conducted in time domain beneath a commercial vehicle chassis. Channel data were collected at the same locations for the car in stationary and in moving status. Stochastic tapped delay line model is used to characterize the channels in both cases. Slightly larger number of multi-path components (MPCs) and mean RMS delay are observed in the moving case. Statistical analysis shows that car movement does not significantly affect the characteristics of UWB channel in the intra-vehicle environment.

1 INTRODUCTION

FCC authorized the unlicensed usage of UWB bandwidth from 3.1GHz to 10.6GHz with restriction on the emission spectrum in 2002 [1]. This greatly stimulated the research interest in the commercial applications of UWB technique. To investigate the UWB signal propagation for the convenience of the system design, a lot of UWB indoor or outdoor channel measurements have been performed in recent years [2] [3] [4] [5]. At the same time, UWB channel models have been proposed by IEEE 802.15.3a and 802.15.4a workgroups to facilitate UWB as a standard wireless communication technique in high data rate short range personal area networks and low cost low power sensor networks [6] [7].

Motivated by the requirement to reduce the weight and the energy consumption of commercial vehicles, it has been proposed to use a wireless network based on UWB technique to replace intra-vehicle sensor cables [8] [9]. Knowledge of UWB channel in such intra-vehicle environment is needed. As mentioned above, most UWB channel data in the literature were measured in indoor, outdoor or industrial environments, which are very different in range and structure from automotives. The barely available investigations on UWB channel in vehicles were performed inside passenger compartment [10] [11], which is not the typical space where vehicle sensors are located.

Because some commercial automotive sensors are located in the engine compartment and some are present at the wheel axes, we conducted the UWB channel measurement inside the engine compartment and beneath the vehicle chassis for a Taurus and an Escalade. Results from our experiments have been published in [12] and [13]. However, those channel data were collected when the cars were stationary in a spacious empty parking building. In order to investigate whether and how car movement influences the channel, we rerun the same set of measurement experiments under the chassis of the Escalade when it is moving on road. This paper compares the measurement result in the car moving case with that of the stationary case. The tapped delay line model is used to describe the UWB multi-path propagation in both cases. Channel model parameters statistically extracted from the collected channel data are compared and analyzed.

2 EXPERIMENT

We conducted the channel measurement in time domain. Narrow UWB pulses of 80 picoseconds as that shown in Figure 1 were generated to sound the channel. The channel sounding equipments used in the experiment include a pulse generator which outputs UWB pulses and a digital oscilloscope (DSO) to record the channel responses. The bandwidth provided by the oscilloscope is as wide as 15GHz and its working sampling rate is set at 40GHz. Two copper scissors-type antennas were installed under the Escalade chassis. One of them was connected with the UWB pulse generator to work as the transmitter (TX) and the other one was connected to the DSO to work as the receiver (RX). The oscilloscope trigger connection was setup to synchronize the transmitter and the receiver.

The measured positions of the antennas in the experiment are illustrated in Figure 2. The transmitting antenna was fixedly installed at the spot TX, below the engine compartment. Figure 3 is a picture showing the transmitting antenna attached to the Escalade chassis from the bottom. The locations of the receiving antenna changed from RX0 to RX9. Among them, the oddly numbered spots are symmetric to the evenly numbered ones across the center line of the chassis. In addition, the distances between neighboring spots are all the same. For each receiving location, ten continuous UWB pulses were

978-1-4244-5239-2/09/$26.00 ©2009 IEEE

generated by the pulse generator at TX to stimulate the channel and their responses were recorded when the car was running around Oakland University campus at a speed between 20 and 45 miles per hour. These continuously generated sounding pulses were separated by more than 100 nanoseconds in time so that their responses did not interfere with each other. Similarly, another ten UWB pulses were generated and their responses were collected while the car was stationary in an empty parking building. When conducting the measurements, there were always line-of-sight (LOS) paths existing between the TX and the RX antennas facing each other.

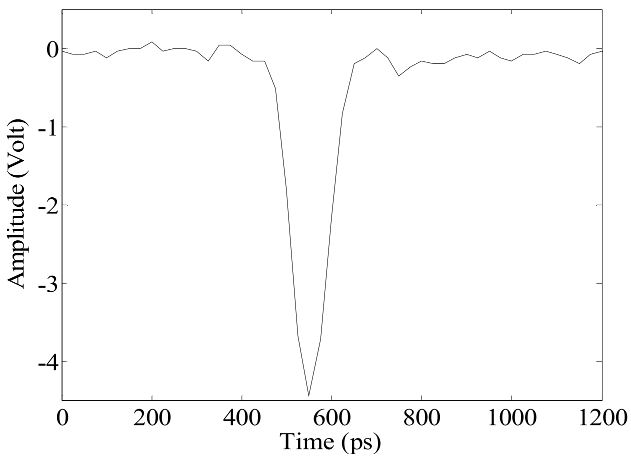

Figure 1. UWB Channel Sounding Pulse

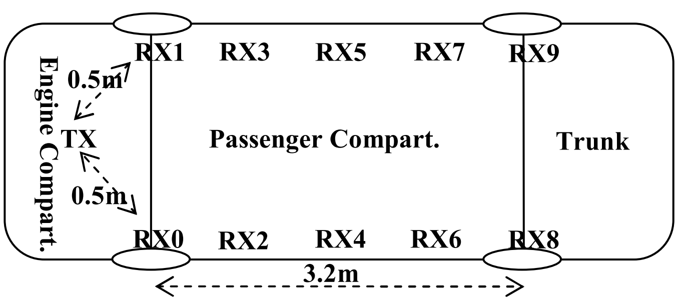

Figure 2. Antenna Locations Beneath the Chassis

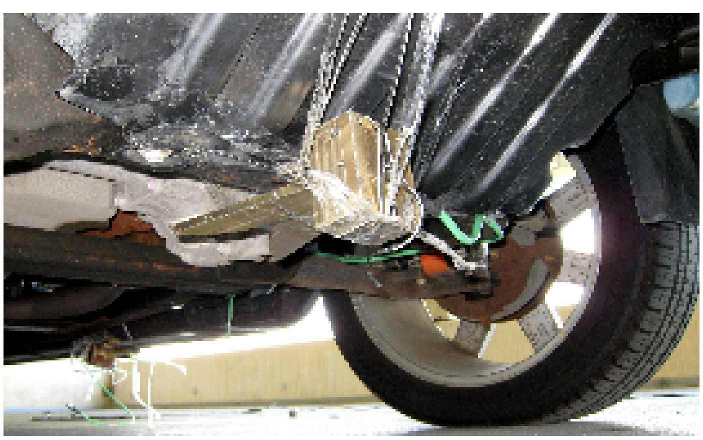

Figure 3. Transmitting Antenna Attached to the Chassis

3 RESULTS

Figure 4 shows two typical examples of the measured multi-path profiles with absolute amplitudes. The upper profile was collected when the car was stationary and the bottom one was from the moving case. Visual inspection reveals that the lengths of both multi-path profiles are less than 10 ns. This is true for all profiles collected at all receiving positions. In addition, the clustering phenomenon which is present in the measurements from indoor or outdoor environments does not exist here. It can also be seen that the shape of the profiles looks very similar to each other. To find out whether the car movement influences the UWB channel, the impulse responses, which characterize the channel, need to be derived for the two cases and compared with each other. The CLEAN algorithm is used to deconvolve the impulse response from each measured data and a tapped delay line model is used to describe them [14] [15].

$$h(t) = \sum_{l=1}^{K} (-1)^{\theta_l} \alpha_l \delta(t - \tau_l) \tag{1}$$

h(t) stands for the multi-path impulse response, K is the number of paths, α_l and τ_l are the positive amplitude and the arrival delay of the *l*-th path. θ_l represents the polarity of the *l*-th path amplitude. For simplicity, it is assumed that θ_l takes the value of 0 or 1 with equal probability. The statistical characteristics of the other model parameters will be described and compared between the vehicle in stationary status and in moving status.

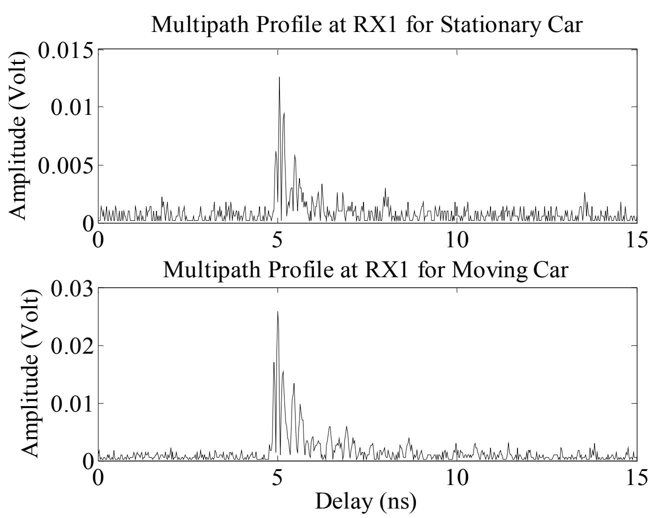

Figure 4. Example of Recorded Multi-path Profiles

3.1 RMS Delay and Number of MPCs

Figure 5 shows the complementary cumulative distribution functions (CCDFs) of the RMS delays from both the stationary case and the moving case, with the mean value of 0.7491 ns or 0.6233 ns as separately marked by the vertical lines. It can be seen that when the car is moving, the RMS delay is slightly larger. Furthermore, the average number of multi-path components calculated from all of the impulse responses is 35 for the stationary vehicle and again a slightly larger number of 42 in the moving case.

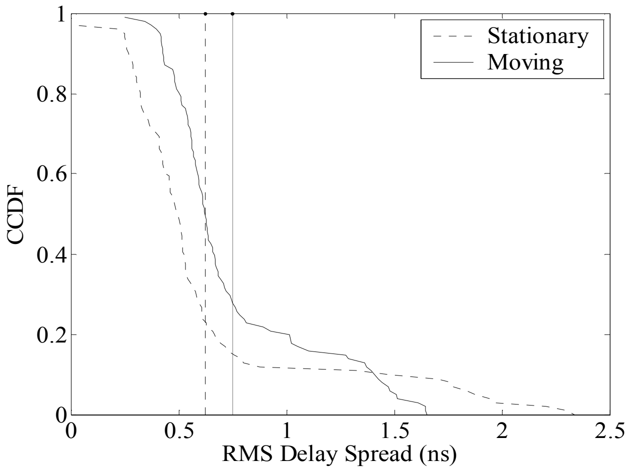

Figure 5. RMS Delay CCDF and the Mean Value

When the car was running on road, the part of the ground covered by the chassis was different each time the measurement was conducted. The slight increase in the number of paths may due to such changes of the ground areas covered by the car which constructed a part of the channel environment. In addition, ground areas on road were normally less smooth than that of the parking building where the stationary measurements were taken. Although the larger RMS delay and number of MPCs indicate a slightly lower data rate to avoid inter-symbol interference due to the movement of the vehicle, the magnitude of the influence is tiny.

3.2 Power Delay Profiles

Power delay profiles (PDPs) illustrate the arrival of power versus time in the impulse responses. Observation of the normalized power delay profiles from all impulse responses reveals that the shape of the PDP always starts with a fast rising edge then decays exponentially from the peak, no matter in the moving or in the stationary case. We take advantage of the following model to describe the PDPs [7] [15]:

$$\overline{\alpha_l^2} = \Omega \cdot [1 - \chi \cdot \exp(-\frac{\tau_l}{\gamma_{rise}})] \cdot \exp(-\frac{\tau_l}{\gamma}) \qquad (2)$$

$\overline{\alpha_l^2}$ is the mean power of the l-th path and Ω stands for the total power of the PDP. The constant χ describes how much the first path is attenuated and larger χ means stronger attenuation. The second constant γ_{rise} decides the steepness of the rising edge and the third constant γ determines the speed of the exponential decay. The larger the values of γ_{rise} and γ are, the sharper the rising and decaying edges are.

The normalized power delay profile averaged over the ten measurement spots from the stationary vehicle is displayed in Figure 6 and its counterpart from the moving vehicle is shown in Figure 7. Their best-fitting curves derived from (2) are found via least square estimation and overlaid in the figures. It can be seen that the average PDP from the moving vehicle has a slightly steeper rising edge and a slightly steeper decaying edge, resulting from a stronger peak path. However, in both cases most power arrives within 2 ns from the first path and the basic shapes of the two average PDPs are similar to each other.

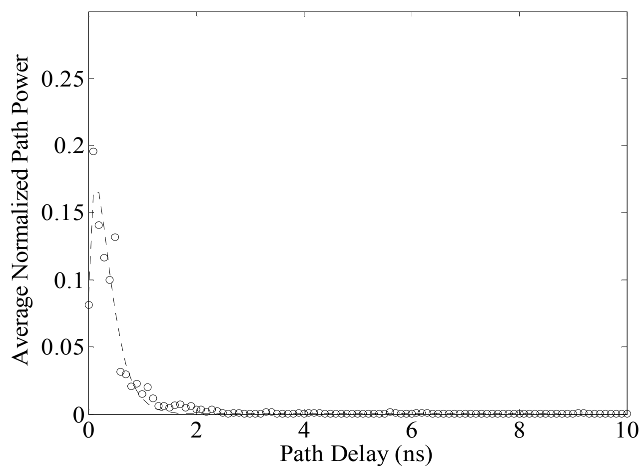

Figure 6. Stationary Vehicle: Average Normalized PDP (χ=0.9108, γ_{rise} =0.4957 ns, γ=0.2311 ns)

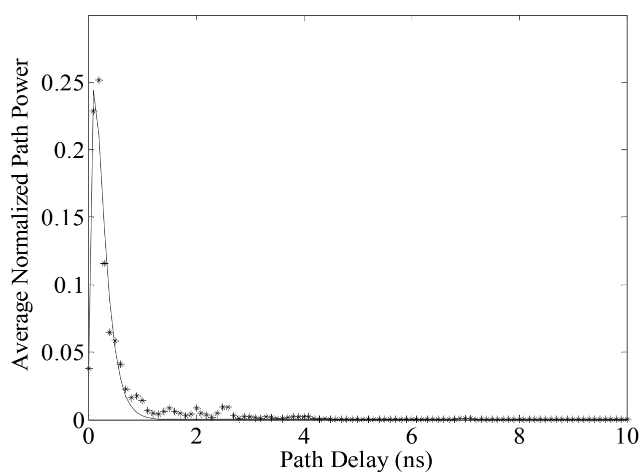

Figure 7. Moving Vehicle: Average Normalized PDP (χ=0.9640, γ_{rise} =0.1874 ns, γ=0.1733 ns)

3.3 Path Arrival

In both the moving vehicle and the stationary vehicle cases, the path arrival is modeled as a Poisson process with a fix rate [6] [7] [15]. As a result, the inter-path arrival intervals observe exponential distribution whose probability density function can be described as below:

$$p(\tau_l \mid \tau_{l-1}) = \lambda \exp[-\lambda(\tau_l - \tau_{l-1})] \qquad (3)$$

where τ_l and τ_{l-1} are the arrival delays of the l-th and the (l-1)-th path relative to the first one, and λ represents the fixed arrival rate of the paths.

Figure 8 shows the CCDFs of the inter-path arrival intervals from the impulse responses of the stationary vehicle and the moving vehicle. It is obvious that the two CCDFs almost coincide with each other when the delay is smaller than 2 ns. In order to quantitatively evaluate the difference, their respective best-fitting exponential distribution curves in the maximum likelihood sense are found and superimposed in the figure. In the stationary vehicle case, the average inter-path interval, which is the reciprocal of the arrival rate λ, equals 0.2228 ns. In comparison, it is 0.2212 ns when the vehicle is moving. Furthermore, for both of them, the arrival intervals larger than 1.5 ns represent less than 1% of all values and they always happen at the tailing parts of the impulse responses. In general, the average inter-path arrival intervals in the two cases almost equal to each other and the movement of the car produces little effect on the path arrival rate.

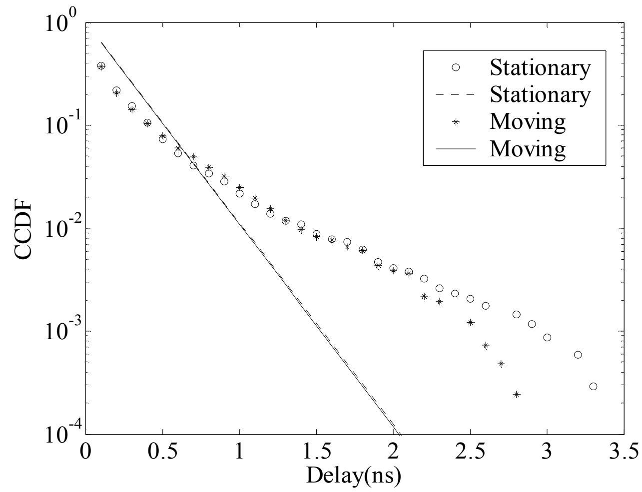

Figure 8. CCDFs of Inter-path Arrival Intervals and the Best-fit Exponential Distribution Curves

3.4 Path Amplitude Distributions

To understand the statistical distribution of the path amplitudes within the impulse responses of the UWB channel in the intra-vehicle environment and to investigate whether the vehicle movement have influences on such distributions, the empirical CDF of the path amplitudes from all normalized impulse responses of the stationary vehicle are calculated. The same calculation is also performed for the moving vehicle and the two resulting CDFs are plotted in Figure 9 and Figure 10 respectively. Visual inspection reveals that the shapes of the two empirical CDF curves are highly similar to each other, indicating that the movement of the vehicle causes little changes to the distribution of the path amplitudes.

In order to find out which distribution function can best describe these cumulative CDF curves, two possible distributions of Rayleigh and lognormal, whose probability density functions (PDF) are listed below, are evaluated.

$$f\_Rayleigh(\alpha) = \frac{\alpha}{\sigma^2}\exp(-\frac{\alpha^2}{2\sigma^2}) \qquad (4)$$

$$f\_Lognormal(\alpha) = \frac{\exp[-\frac{(\ln(\alpha)-\mu)^2}{2\sigma^2}]}{x\sigma\sqrt{2\pi}} \qquad (5)$$

In the above functions, σ is the standard deviation and μ is the expected value. Values of these parameters are found by matching both distributions against the two empirical CDF curves and by finding the best-fitting ones via maximum likelihood estimation. Figure 9 overlays the best-fitting Rayleigh and lognormal distributions with the cumulative CDF of the path amplitudes for the stationary vehicle and Figure 10 is for the vehicle in movement. It can be seen that in each case, lognormal distribution is almost a perfect fit for the path amplitude distribution. In addition, the movement of the vehicle only causes slight changes to the values of the best-fitting lognormal distribution parameters б and μ, as illustrated in Figure 10 and Figure 9. This verifies the conclusion from the visual inspection mentioned above.

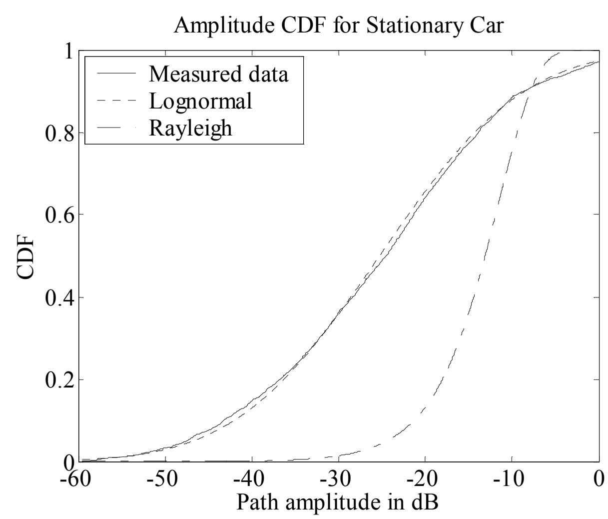

Figure 9. Best-fitting Lognormal and Rayleigh for Path Amplitudes CDF from Stationary Vehicle (Rayleigh: б=0.1881, Lognormal: б=13.0571 and μ= -25.2768)

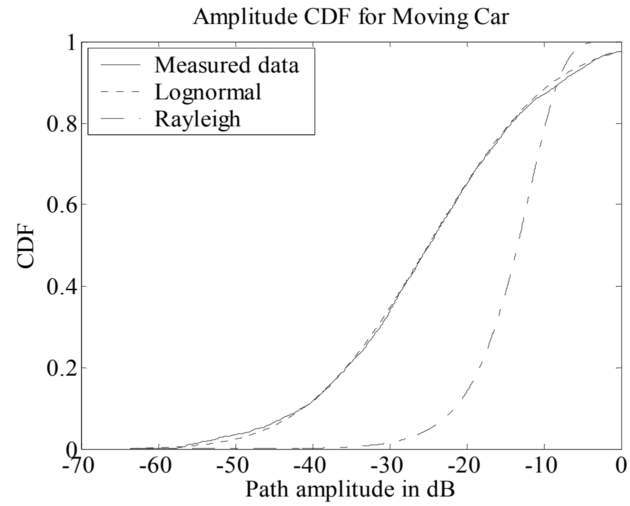

Figure 10. Best-fitting Lognormal and Rayleigh for Path Amplitudes CDF from Moving Vehicle (Rayleigh: σ=0.1813, Lognormal: σ=12.6417 and μ= -24.9959)

4 SUMMARY

UWB propagation measurements have been conducted beneath the chassis of a commercial vehicle from time domain by sounding the channel with pulses of 80 picoseconds. Ten responses, each of length 15 nanoseconds, have been recorded by a DSO at each of ten measurement locations when the vehicle is stationary. Same measurements have been repeated when the vehicle moves at a speed between 20 miles and 45 miles per hour.

The stochastic tapped delay line model has been used to model the UWB channel in the above measurement environment and statistical model parameters have been derived from the measured data of the vehicle in both stationary and movement status. Comparison of the parameter values shows that the movement of the vehicle leads to only slight increase in the RMS delay and the number of MPCs as well as very slight changes in the average power delay profile, in the path arrival and the path amplitude distribution. In conclusion, movement of the vehicle causes very little influence on the UWB propagation beneath the chassis. This result indicates that the movement of the vehicle does not require special considerations when designing the UWB system working beneath the chassis and the same UWB system can work without change or adjustment no matter the vehicle is stationary or in movement.

5 ACKNOWLEDGMENT

The authors appreciate General Motors Corporation for sponsoring this research and for providing the measurement vehicle. Acknowledgment also goes to Michael Corrigan and Asia Walton for their help when conducting the experiment.

REFERENCES

[1] FCC, First Report and Order 02-48. February 2002.

[2] D. Cassioli, M. Z. Win and A. F. Molisch, “The ultra-wide bandwidth indoor channel: from statistical model to simulations,” *IEEE Journal on Selected Areas in Communications*, vol. 20, No. 6, pp. 1247-1257, Aug. 2002.

[3] S.S. Ghassemzadeh, R. Jana, C.W. Rice, W. Turin, V. Tarokh, “Measurement and modeling of an ultra-wide bandwidth indoor channel,” *IEEE Transactions on Communications*, Vol. 52, No. 10, pp. 1786-1796, Oct 2004.

[4] J. Karedal, S. Wyne, P. Almers, F. Tufvesson, and A. F. Molisch, “Statistical analysis of the UWB channel in an industrial environment,” *2004 IEEE 60th Vehicular Technology Conference (VTC 2004)*, vol. 1, pp. 81-85, Sep. 2004.

[5] M. D. Renzo, F. Graziosi, R. Minutolo, M. Montanari and F. Santucci, “The ultra-wide bandwidth outdoor channel: from measurement campaign to statistical modeling,” *Mobile Networks and Applications*, vol. 11, no. 4. pp. 451-467, Aug. 2006.

[6] J. Foerster, “Channel modeling sub-committee report final,” IEEE P802.15-02/490r1-SG3a, Feb. 2003.

[7] A. F. Molisch, *et al*, “IEEE 802.15.4a channel model - final report,” IEEE 802.15-04-0662-00-004a, Nov. 2004.

[8] T. ElBatt, C. Saraydar, M. Ames and T. Talty, “Potential for intra-vehicle wireless automotive sensor networks,” *2006 IEEE Sarnoff Symposium*, Mar. 2006.

[9] J. Li and T. Talty, "Channel characterization for ultra-wideband intra-Vehicle sensor networks," *2006 IEEE Military Communications Conference (MILCOM 2006)*, Oct. 2006.

[10] P. C. Richardson, W. Xiang, and W. Stark, “Modeling of ultra-wideband channels within vehicles”, *IEEE Journal on Selected Areas in Communications*, vol. 24, pp. 906-912, Apr. 2006.

[11] W. Xiang “A vehicular ultra-wideband channel model for future wireless intra-vehicle communications (IVC) systems,” *2007 IEEE 66th Vehicular Technology Conference (VTC 2007),* pp.2159-2163, Sep. 2007.

[12] W. Niu, J. Li and T. Talty, “Intra-vehicle UWB channel measurements and statistical analysis,” *2008 IEEE Global Telecommunications Conference (GLOBECOM 2008)*, Nov. 2008.

[13] W. Niu, J. Li and T. Talty, "Ultra-wideband channel modeling for intra-vehicle environment," *EURASIP Journal on Wireless Communications and Networking*, vol. 2009, Article ID 806209, 12 pages, 2009.
[14] R. G. Vaughan and N. L. Scott, “Super-resolution of pulsed multi-path channels for delay spread characterization,” *IEEE Transactions on Communications*, vol. 47, pp. 343-347, Mar. 1999.
[15] A. F. Molisch, “Ultrawideband propagatiton channels-theory, measurement, and modeling,” *IEEE Transactions on Vehicular Technology*, vol. 54, No. 5, pp. 1528-1545, Sep. 2005.